Upper and lower critical magnetic fields of superconducting NdFeAsO$_{1-x}$F$_x$ single crystals studied by Hall-probe magnetization and specific heat

Z. Pribulova,[1,2] T. Klein,[1,3] J. Kacmarcik,[2,4] C. Marcenat,[4] M. Konczykowski,[5] S. L. Bud'ko,[6] M. Tillman,[6] and P. C. Canfield[6]

[1]*Institut Néel, CNRS, BP 166, 38042 Grenoble Cedex 9, France*
[2]*Centre of Low Temperature Physics, IEP, SAS and FS, UPJŠ, Watsonova 47, 043 53 Košice, Slovakia*
[3]*Institut Universitaire de France and Université Joseph Fourier, BP 53, 38041 Grenoble Cedex 9, France*
[4]*Institut Nanosciences et Cryogénie, SPSMS-LATEQS, CEA, 17 rue des Martyrs, 38054 Grenoble Cedex 9, France*
[5]*Laboratoire des Solides Irradiés, Ecole Polytechnique, 91128 Palaiseau, France*
[6]*Department of Physics and Astronomy, Ames Laboratory, Iowa State University, Ames, Iowa 50011, USA*

The upper and lower critical fields have been deduced from specific heat and Hall-probe magnetization measurements in nonoptimally doped Nd(O,F)FeAs single crystals ($T_c \sim 32-35$ K). The anisotropy of the penetration depth (Γ_λ) is temperature independent and on the order of 4.0 ± 1.5. Similarly specific-heat data lead to an anisotropy of the coherence length $\Gamma_\xi \sim 5.5 \pm 1.5$ close to T_c. Our results suggest the presence of rather large thermal fluctuations and the existence of a vortex liquid phase over a broad temperature range (~ 5 K large at 2 T).

PACS number(s): 74.25.Ha, 74.25.Fy, 74.25.Nf, 74.25.Op

The recent discovery of superconductivity at unusually high temperature (up to 56 K) in rare-earth iron oxypnictides[1,2] has been the focus of a tremendous number of theoretical and experimental works in the past few months. The possible coexistence of superconductivity with a complex magnetic structure[3] makes this system particularly fascinating and a nonconventional pairing mechanism (associated with multigap superconductivity in electron and hole pockets) has been suggested by different groups.[4] In this context, it is very important to have a precise determination of the temperature dependence of the critical fields and corresponding anisotropies.

We will focus on the superconducting properties of the NdFeAs(O,F) compound.[5] The aim of this Rapid Communication is to present combined Hall-probe magnetization and specific-heat (C_p) measurements performed on Nd-doped single crystals. A superconducting anomaly was clearly visible in C_p around 35 K and, as previously observed in high-T_c oxides, this anomaly is symmetric and broad and rapidly collapses as the magnetic field is increased. On the other hand, the lower critical field presents a classical temperature dependence for both $H_a \| c$ and $H_a \| ab$ [with $H_{c1}^c(0) \sim 120 \pm 30$ G and $H_{c1}^{ab} \sim 40 \pm 10$ G] and the anisotropy of the penetration depth remains on the order of 4 on the entire temperature range. A similar anisotropy is obtained for the upper critical field from the C_p measurements.

NdFeAs(O,F) samples have been synthesized at high pressure in a cubic multianvil apparatus. More details of the synthesis are given elsewhere.[6] Both Hall-probe magnetization and C_p measurements have been performed on the same plateletlike single crystals extracted from the polycrystalline batch [with dimensions of $\sim 100 \times 100 \times 30$ μm^3 (sample 1), $\sim 120 \times 80 \times 30$ μm^3 (sample 2), and $\sim 170 \times 100 \times 50$ μm^3 (sample 3)].

The local magnetization of the platelet has been measured by placing the sample on the top of an array of miniature Hall probes of dimensions 4×4 or 8×8 μm^2. The ac trans-mittivity (T'_{ac}, related to the *local susceptibility*) has been measured by applying a small (~ 1 G) ac field and recording the corresponding response of the probe as a function of the temperature [see Fig. 1(a)]. T'_{ac} is obtained by subtracting the response in the normal state from the data and is rescaled to -1 at $T=4.2$ K (due to the small but nonzero distance between the probe and the sample surface, about 10% of the external field is still picked up by the probe in the superconducting state). As shown in Fig. 1(a), the transmittivity measured in the center of the sample first presents a small paramagnetic increase starting at ~ 37 K followed by a sharp diamagnetic jump at $T \sim 34$ K (sample 1). This paramagnetic bump (also observed in zero-field-cooled dc measurements) reflects a nonhomogeneous distribution of the field[7] between 34 and 37 K. However, the presence of a clear anomaly in the specific heat emphasizes the overall good quality of the platelets. A similar bump has been observed in sample 2 between 34.5 and 37.5 K and in sample 3 between 36.5 and 37.5 K. Note also that previous global magnetization measurements[8] yield to an onset of the diamagnetic response of the polycrystalline batch around $T \sim 51$ K, in agreement with a resistivity T_c on the order of 50 K for optimally doped samples.[5] We did not find any sign of superconductivity around 51 K in our platelets, indicating that the diamagnetic response observed above 40 K in global measurements is due to a distribution of T_c values (i.e., F content) within the polycrystalline batch.

Specific-heat measurements have been performed on the same crystallites (samples 1 and 2) using an ac technique. This high-sensitivity technique (typically 1 part in 10^4) is very well adapted to measuring C_p of very small samples. Heat was supplied to the sample at a frequency $\omega=10$ Hz by a light-emitting diode via an optical fiber. The temperature oscillations have been recorded with a thermocouple which has been calibrated from measurements on ultrapure silicon. The superconducting contribution to the specific heat (ΔC_p) has been obtained by subtracting the curve at $\mu_0 H_a = 7$ T
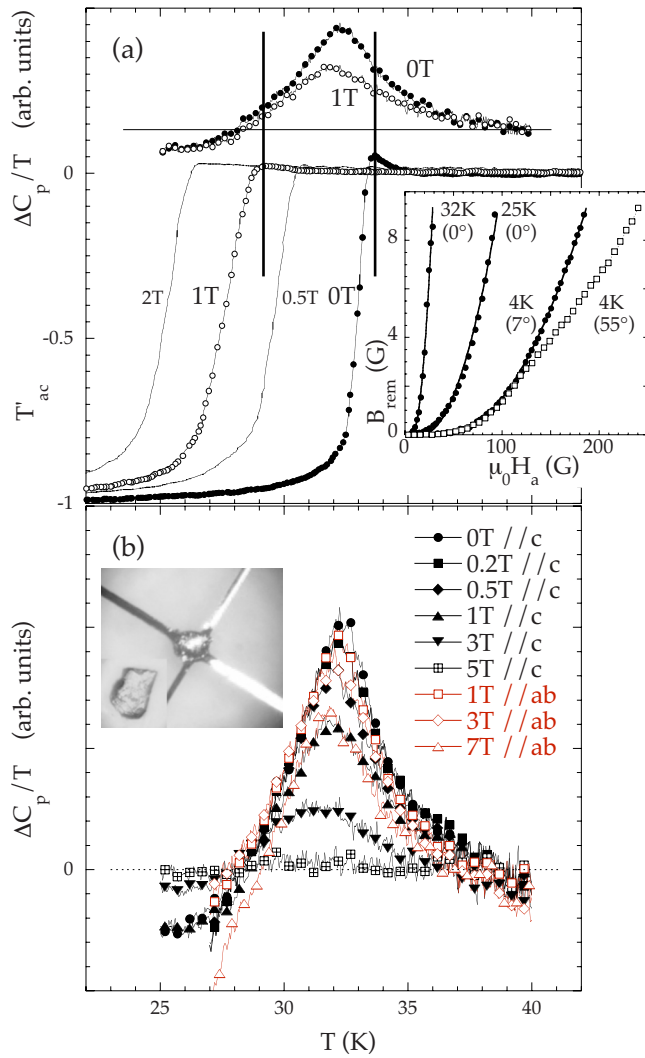
FIG. 1. (Color online) (a) Temperature dependence of the ac transmittivity and specific heat in a non-optimally doped Nd(F,O)FeAs platelet (sample 1) for the indicated field values ($H_a \| c$). In the inset: Remanent field (B_{rem}) as a function of the applied field $\mu_0 H_a$ (see text for details) for the indicated temperatures and field orientation. The solid lines are $(H_a - H_p)^2$ fits to the data. (b) Temperature dependence of the specific heat in a non-optimally doped Nd(F,O)FeAs platelet (sample 1) for $H_a \| c$ (closed black symbols) and $H_a \| ab$ (open red symbols) for the indicated field values. The inset shows sample 1 mounted on the thermocouple cross, for which the width of the legs is ≈ 50 μm, as well as for sample 3 (bottom left corner).

(for $H_a \| c$) from the curves obtained for lower fields as well as a $(H_a/T)^2$ contribution to account for the presence of a magnetic background. As shown in Fig. 1(b) (sample 1), there is no sharp discontinuity at T_c and the anomaly has the shape of a rounded peak with a height on the order of a few 10^{-3} of the total specific heat. The other striking behavior is the influence of the magnetic field. As previously observed in cuprates,[9] the smearing of the anomaly with field is unexpectedly strong with an almost field-independent onset. The maximum of C_p is pushed downward in temperature by the field with a characteristic average slope on the order of -2 T/K for $H_a \| c$ and -7 T/K for $H_a \| ab$ (compared to
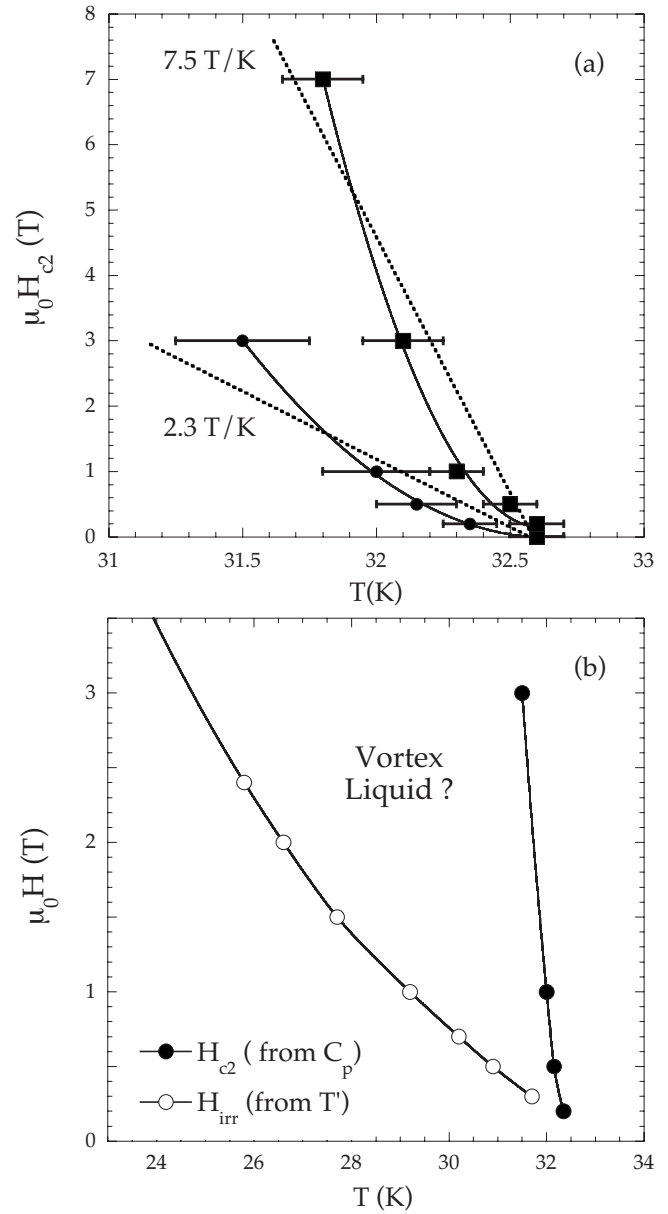

FIG. 2. (a) Temperature dependence of the upper critical field [maximum of the specific-heat anomaly; see Fig. 1(a)] for $H_a \| c$ (circles) and $H_a \| ab$ (squares). (b) Comparison between H_{c2} (deduced from C_p, closed symbols) and the onset of the diamagnetic response H_{irr} (open symbols) for $H_a \| c$ suggesting the existence of a broad vortex liquid phase.

-1.5 and -9 T/K, respectively, in optimally doped YBaCuO; note that the shift is possibly nonlinear for small magnetic field and see solid line in Fig. 2 and discussion below). As in cuprates, the shape of the anomaly precludes any precise determination of H_{c2}. However, assuming that H_{c2} is close to the maximum of C_p (H_{max}) and taking the corresponding linear temperature dependence, we hence get $H_{c2}(0) \sim 0.7 \times dH_{max}/dT \times T_c \sim 40$ and ~ 170 T for $H_a \| c$ and $H_a \| ab$, respectively. The corresponding anisotropy of the coherence length $\Gamma_\xi = \xi_c/\xi_{ab} = \Gamma_{H_{c2}}$ is hence on the order of $H_{c2}^{ab}(0)/H_{c2}^c(0) \sim 4$. The uncertainty on the H_{c2} values is rather large but Γ_ξ can also be estimated from the total shape

of the anomaly, writing $\Delta C(\Gamma_\xi \times H_a \| ab) \sim \Delta C(H_a \| c)$, consistently leading to $\Gamma_\xi \sim 5.5 \pm 1.5$. This value is also in good agreement with the one previously reported by Welp *et al.*[10] and with recent band-structure calculations.[11]

The influence of H_a on the C_p anomaly and its overall shape is strikingly different from the one observed in classical superconductors or even in the $(K, Ba)BiO_3$ system ($T_c \sim 32$ K) (Ref. 12) or MgB_2 ($T_c \sim 39$ K) (Ref. 13) of similar T_c values. It is tempting to attribute these deviations to fluctuation effects. To reinforce this idea, it is worth noting that the onset of the diamagnetic response well coincides with the inflection point of the C_p anomaly for $H_a = 0$ but is pushed toward substantially lower temperature in field (~ 5 K lower than the C_p shift for $\mu_0 H_a = 2$ T). As T'_{ac} is sensitive to pinning, this result suggests that the irreversibility line is well separated from the superconducting transition for $H_a \neq 0$ (see inset of Fig. 2(b) for $H_a \| c$; a similar result—not shown—is obtained for $H_a \| ab$), supporting the idea of an extended vortex liquid phase. The importance of thermal fluctuations can be quantified by the Ginzburg number[14] $G_i = (k_B T_c / \epsilon_0 \xi_c)^2 / 8$, where $\epsilon_0 \left[= (\Phi_0 / 4\pi\lambda_{ab})^2 \right]$ is the line tension of the vortex matter. Large λ values (see below) combined with small ξ values hence lead here to $\epsilon_0 \xi_c \sim 200$ K (i.e., similar to cuprates) compared to ~ 1000 K in $(K, Ba)BiO_3$ and even $\sim 10^4$ in MgB_2. Although smaller than in cuprates due to smaller T_c values, thermal fluctuations are hence expected to play a role in this system possibly leading to the melting of the vortex solid ($G_i \sim 3 \times 10^{-3} - 10^{-2}$). A similar conclusion was drawn by Welp *et al.*[10] Note that, as expected for vortex melting, the irreversibility line clearly presents a positive curvature $[H_{irr} \propto (1 - T/T_c)^\alpha$ with $\alpha \sim 1.5$; for a review see Ref. 14]. Similarly, thermal fluctuations may also induce an upward curvature in the H_{c2} line[15] but even though our data suggest the existence of such a curvature (see also Ref. 10), we cannot unambiguously conclude given the uncertainties and limited temperature range of the C_p data.

The first penetration field H_p has been deduced by measuring the remanent field (B_{rem}) in the sample after applying an external field H_a and sweeping the field back to zero. For $H_a < H_p$ no vortices penetrate the sample and the remanent field remains equal to zero. H_a is progressively increased until a finite remanent field is obtained as vortices remain pinned in the sample for $H_a > H_p$ [B_{rem} increasing as $(H_a - H_p)^2$; see solid line in the inset of Fig. 1(a)]. Theoretically speaking, H_p is expected to depend on the position of the probe, being larger in the center of the sample as vortices first remain pinned close to sample edges. However, experimentally, a nonzero B_{rem} value could be detected almost simultaneously on all the probes due to the nonzero distance between the sample and the probe. Note that we did not observe any significant change in the $B_{rem}(H_a)$ curve up to $H_a \sim 3H_p$ as the magnetic field was tilted away from the c axis (with an angle $\theta_{H_a} \leq 60° - 70°$). Even though the angle between the internal field (θ_H) and the c axis is reduced by the demagnetization effects, this surprising behavior suggests that the induction (B) in the sample remains perpendicular to the platelets up to large θ_H values [see inset of Fig. 1(a) for sample 1 at $\theta_{H_a} = 7°$ and $55°$]. B_{rem} finally decreases with θ for $H_a \gtrsim 3H_p$ (and/or for $\theta_{H_a} \gtrsim 70°$), indicating that the vortices finally align on the applied field for large H_a (and/or θ_{H_a}) values.
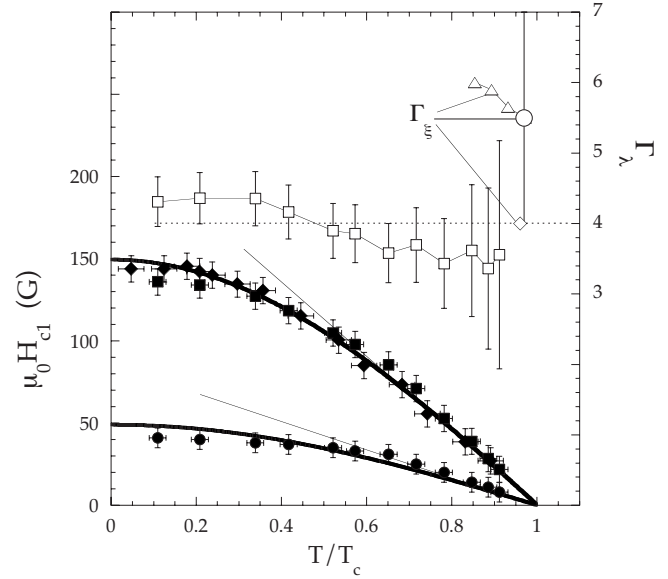

FIG. 3. Temperature dependence of the lower critical field H_{c1} along the c direction (solid squares for sample 3 and solid lozenges for sample 1, rescaled by a factor of 1.5) and ab plane for sample 3 (solid circles). The solid lines are the standard behaviors expected from the BCS theory. The corresponding temperature dependence of the anisotropy ($\Gamma_\lambda = 1.3 \times \Gamma_{H_{c1}}$) is also reported (open squares). The error bars correspond to the uncertainties on the determination of H_p; the whole curve might be shifted ± 1.5 due to the uncertainty of the demagnetization factor. In all cases, Γ_λ remains flat in T. The Γ_ξ values deduced from C_p (present work: open circles; Ref. 10: open lozenge) and transport (Ref. 27; open triangles) measurements are also displayed.

In samples with rectangular cross sections, flux lines partially penetrate into the sample through the sharp corners even for $H_a < H_p$ (Refs. 16 and 17) but remain "pinned" at the sample equator. The magnetization at $H_a = H_p$ is then larger than H_{c1} and the standard "elliptical" correction for H_{c1} [$= H_p / (1 - N)$, where N is the demagnetization factor] cannot be used anymore. Following Ref. 16, in the presence of geometrical barriers, H_p is related to H_{c1} through $H_{c1} \approx H_p / \tanh(\sqrt{\alpha d / 2w})$, where α varies from 0.36 in strips to 0.67 in disks ($2w$ and d being the sample width and thickness, respectively). Taking an average α value of ~ 0.5,[18] we hence got[19] $H_{c1}^c(0) \sim 110 \pm 20$ G in sample 1, $H_{c1}^c(0) \sim 100 \pm 20$ G in sample 2, and $H_{c1}^c(0) \sim 140 \pm 30$ G in sample 3. To obtain H_p in the ab plane, sample 3 has been rotated by 90° putting the probe on the small side of the sample [i.e., applying H_a along the long direction of the sample so that $H_p^{ab}(0) \sim H_{c1}^{ab}$]. We hence obtained $H_{c1}^{ab} \sim 40 \pm 10$ G (in sample 3).

The temperature dependence of H_{c1} for both $H_a \| c$ (samples 1 and 3; the data for sample 1 have been rescaled by a factor of 1.5) and $H_a \| ab$ (sample 3) is displayed in Fig. 3. As shown, H_{c1}^c clearly flattens off at low temperatures (down to 1.6 K for sample 1), indicating that the gap is fully open in our NdAsFe(O,Fe) single crystals. This result is in striking contrast with H_p measurements in Ref. 21, which suggested that H_{c1} varies linearly at low temperature in LaFeAs(O,F), hence suggesting the existence of gapless su-

perconductivity. On the other hand, a very similar temperature dependence [and $H_{c1}(0)$ values] was recently obtained by Okazaki *et al.*[22] in Pr-doped samples.

The lower critical field is related to the penetration depth through $H_{c1}^c = \Phi_0^2/(4\pi\lambda_{ab}^2)[Ln(\kappa)+c(\kappa)]$, where $\kappa = \lambda_{ab}/\xi_{ab}$ (ξ being the coherence length) and $c(\kappa)$ is a κ-dependent function tending toward ~ 0.5 for large κ values. Taking $H_{c2}^c(0) \sim 40$ T, one gets $\lambda_{ab}(0) \sim 270 \pm 40$ nm.[23] Those λ values are consistent with those previously obtained in oxypnictides. Indeed, slightly lower λ_{ab} values (~ 200 nm) have been reported in both Sm- and Nd-doped samples with higher T_c (~ 50 K, from either torque,[20] muon relaxation,[24] or plasma frequency[25] measurements), whereas $\lambda \sim 360-390$ nm have been obtained in La-doped samples with lower T_c values [~ 23 K (Refs. 21 and 26)].

For $H\|ab$, $H_{c1}^{ab} = \Phi_0^2/(4\pi\lambda_{ab}\lambda_c)[Ln(\kappa^*)+c(\kappa^*)]$, with $\kappa^* = \lambda_c/\xi_{ab}$, and $H_{c2}^{ab} = \Phi_0^2/(2\pi\xi_c\xi_{ab}) \sim 170$ T, leading to $\lambda_c \sim 1200 \pm 200$ nm and a corresponding anisotropy (Γ_λ) on the order of 4.0 (± 1.5), almost temperature independent down to 1.6 K (see Fig. 3, sample 3, $\Gamma_\lambda = \Gamma_{H_{c1}} \times \{1+Ln(\Gamma_\lambda)/[Ln(\kappa)+0.5]\} \sim 1.3 \times \Gamma_{H_{c1}}$). Note that our data are in striking contrast with those deduced from torque measurements in Sm-doped samples[20] which led to strongly increasing Γ_λ values, exceeding 30 at low temperature. On the other hand, our Γ_λ consistently tends toward Γ_ξ for $T \to T_c$ deduced either from C_p (present work and Ref. 10) or transport data.[27] The difference between the anisotropies measured at low (Γ_λ) and high (Γ_ξ) fields remains within our error bars and we hence cannot comment on a possible similarity with MgB_2 in which the coexistence of two gaps leads to a strong field and temperature dependence of the anisotropy.[28]

In conclusion, specific heat and Hall-probe magnetization data suggest that $\Gamma_\xi \sim \Gamma_\lambda \sim 5 \pm 2$ in NdFeAs(F,O) single crystals. Whereas the irreversibility rapidly shifts toward lower temperature for increasing H_a, the C_p anomaly collapses and shows only a minor shift, suggesting the presence of strong thermal fluctuations possibly leading to the melting of the vortex solid.

[1] Y. Kamihara *et al.*, J. Am. Chem. Soc. **130**, 3296 (2008).

[2] C. Wang *et al.*, EPL **83**, 67006 (2008).

[3] See, for instance, C. de la Cruz *et al.*, Nature (London) **453**, 899 (2008); A. J. Drew *et al.*, Phys. Rev. Lett. **101**, 097010 (2008); Z. S. Wang *et al.*, Phys. Rev. B **78**, 140501(R) (2008); S. Kitao *et al.*, J. Phys. Soc. Jpn. **77**, 103706 (2008).

[4] L. Boeri *et al.*, Phys. Rev. Lett. **101**, 026403 (2008); I. I. Mazin *et al.*, *ibid.* **101**, 057003 (2008).

[5] Z. A. Ren *et al.*, EPL **82**, 57002 (2008).

[6] M. Tillman *et al.* (unpublished).

[7] N. Avraham *et al.*, Phys. Rev. B **77**, 214525 (2008).

[8] R. Prozorov *et al.*, arXiv:0805.2783 (unpublished).

[9] A. Carrington *et al.*, Phys. Rev. B **55**, R8674 (1997), and references therein.

[10] U. Welp *et al.*, Phys. Rev. B **78**, 140510(R) (2008).

[11] D. J. Singh and M. H. Du, Phys. Rev. Lett. **100**, 237003 (2008).

[12] S. Blanchard *et al.*, Phys. Rev. Lett. **88**, 177201 (2002).

[13] L. Lyard *et al.*, Phys. Rev. B **66**, 180502(R) (2002).

[14] G. Blatter *et al.*, Rev. Mod. Phys. **66**, 1125 (1994).

[15] T. Klein *et al.*, Phys. Rev. Lett. **92**, 037005 (2004).

[16] E. H. Brandt, Phys. Rev. B **59**, 3369 (1999).

[17] E. Zeldov *et al.*, Phys. Rev. Lett. **73**, 1428 (1994).

[18] A detailed analysis on MgB_2 samples showed that all measured samples fell within those two (strips and disks) limits; L. Lyard, T. Klein, J. Marcus, R. Brusetti, C. Marcenat, M. Konczykowski, V. Mosser, K. H. Kim, B. W. Kang, H. S. Lee, and S. I. Lee, Phys. Rev. B **70**, 180504(R) (2004).

[19] Note that for the rather high $d/2w$ ratio of our platelets a standard "elliptical" correction would only slightly overestimate H_{c1}: for samples 1 and 2 $d/2w \sim 0.3$, leading to $1/(1-N) \sim 4.0 \pm 0.2$ for strips and 2.8 ± 0.2 for disks compared to $H_{c1}/H_p \sim 2.7 \pm 0.4$ for geometrical corrections.

[20] S. Weyeneth *et al.*, arXiv:0806.1024 (unpublished).

[21] C. Ren *et al.*, arXiv:0804.1726 (unpublished).

[22] R. Okazaki *et al.*, arXiv:0811.3669 (unpublished).

[23] Our H_{c2} values are significantly higher than those reported in Ref. 10 but lower than those previously reported from transport measurements [see Ying Jia, Peng Cheng, Lei Fang, Huiqian Luo, Huan Yang, Cong Ren, Lei Shan, Changzhi Gu, and Hai-Hu Wen, Appl. Phys. Lett. **93**, 032503 (2008); C. Senatore *et al.*, Phys. Rev. B **78**, 054514 (2008)]; however, a change by a factor 2 of H_{c2} induces a change in λ of less than 10%.

[24] A. J. Drew *et al.*, arXiv:0805.1042, Phys. Rev. Lett. (to be published); R. Khasanov *et al.*, Phys. Rev. B **78**, 092506 (2008).

[25] A. Dubroka *et al.*, Phys. Rev. Lett. **101**, 097011 (2008).

[26] H. Luetkens *et al.*, Phys. Rev. Lett. **101**, 097009 (2008).

[27] Y. Jia *et al.*, Supercond. Sci. Technol. **21**, 105018 (2008).

[28] L. Lyard *et al.*, Phys. Rev. Lett. **92**, 057001 (2004).